Journal of Basrah Researches (Sciences) **50**(1), 62 (2024)
DOI: https://doi.org/10.56714/bjrs.50.1.6

Theoretical Study for Spin Transport properties of FM-(G/C)10- FM

Mohannad A. Merzoq, Jenan M. Al-Mukh*

Department of Physics, College of Education for Pure Sciences, University of Basrah, Basrah, Iraq

ARTICLE INFO

Received 25 November 2023
Accepted 13 February 2024
Published 30 June 2024

Keywords:

Spin Transport of (G/C)10, Ferromagnetic Leads, Spin filtering, spin switching**,** spin blockade

Citation: M.A. Merzoq, J.M. Al-Mukh, J. Basrah Res. (Sci.) **50**(1), 62 (2024). DOI:https://doi.org/10.56714/bjrs.50.1.6

ABSTRACT

In the present study, we propose a physical model to study spin transport through DNA system and provide apparent physical mechanism for spin dependent phenomenon. The system considered in our work is DNA bases guanine-cytosine coupled to two ferromagnetic leads (FM-(G/C)10-FM) in parallel and anti-parallel configuration case, throughout magnetic quantum contacts. Our treatment is based on the tight binding model to derive obvious formula for the transmission spectrum which is employed to investigate the spin dependent current-bias voltage characteristics and the temperature - Conductance dependence. Our calculations of for strong, weak and without backbone regimes. Various factors are involved in our -study. These are the electrical contacts between DNA molecules and electrodes, the structure of DNA molecule and the environment around DNA molecule. The system spin dependent factors, that are investigated extensively in our study include the spin dependent coupling between subsystems, the quantum contacts between active region and electrodes, majority and minority electrons spin in the ferromagnetic leads as well as externally applied bias voltage. Variation of these factors can enhanced or suppressed spin transport through (G/C)10 molecule. The transmission spectrum calculations conform that the spin transport throughout (G/C)10 originates by a coherent tunneling process between neighboring bases through the overlapping of the LUMO orbitals of the bases. Our results showed that the spin-polarized transport that can be effectively regulated by the type of regime as well as the spin configuration in the leads which can exhibit efficient spin filtering and spin switching by employing the spin blockade phenomenon.

1. Introduction

We Molecular electronic devices have been extensively studied in recent years with regard to their potential applications in nanoscale devices and spintronics. Due to their small size and low power consumption, many basic devices utilizing molecules had been demonstrated including tunnel junctions with negative differential resistance, rectifiers, amplifiers and data storage[1]**.** The trend towards smaller electronic devices is driving the nanoscale electronics to its ultimate molecular-scale limit, which offers

***Corresponding author email :** www.montader1999.mm@gmail.com

ISSN: 1817-2695 (Print); 2411-524X (Online)
Online at: https://jou.jobrs.edu.iq

the possibility of exploiting quantum effects. The rich phenomena that have been discovered in these areas arise from mixing of electronic energies in the molecule with external macroscopic structures. [2]. The Spintronics, involves the study of active control and manipulation of spin degrees of freedom in solid-state systems. The primary focus was on the basic physical principles underlying the generation of carrier spin polarization, spin dynamics, and spin-polarized transport in semiconductors and metals. Spintronics systems exploit the fact that the electron current is composed of spin-up and spin-down carriers, which carry information encoded in their spin state and interact differently with magnetic materials[13]**.** Based on experimental motivations, electrical measurements were mostly performed for dried DNA molecules that are connected to metal electrodes. As the size of DNA molecule is known to be 2 nm in diameter it may be possible to fabricate the smaller electrical circuits than conventional one such as conductive wire and switching devices[4-5]. Recent experiments have demonstrated double-stranded DNA molecules as efficient spin filters at room temperature Generally speaking the spin sensitivity of organic spintronics devices is basically related to the magnetic properties of the organic material or those of the electrodes where the molecules is attached[6].
The goals of our work can be summarized as following:
1- Calculating the spin dependent energy spectrum of (G/C)10 that must be utilized to calculate the spin dependent transmission spectrum of the active region.
2- Calculating the spin dependent transport properties to obtain the fundamental understanding of the impact of every factor involved in our work on the characteristics of (G/C)10.
3- Analyzing our results and determining the recommendations for the use of FM-(G/C)10-FM in the field of spintronics applications.

2. The Theoretical Model

We describe the system under consideration (that shown in fig. (1) by spin-dependent Hamiltonian (using Dirac's notations). This electronic Hamiltonian takes into account all the sub-systems interactions. The different indexes D, A, a, L and R denote the donor, acceptor, the active region and the left lead and right leads.

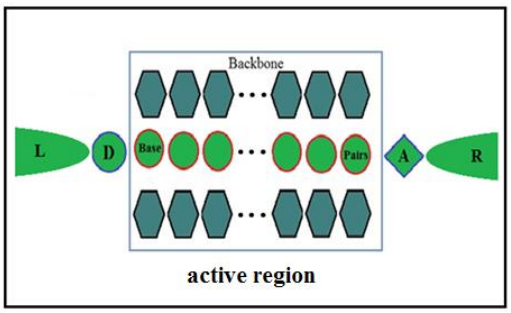

Fig.1. The fishbone model for DNA. The active region contains base pairs and backbone

By using the tight binding model, the spin dependent Hamiltonian model for certain spin is written as follows:

$$\begin{aligned}\widehat{H} = {} & E_D^\sigma |D\sigma\rangle\langle D\sigma| + E_A^\sigma |A\sigma\rangle\langle A\sigma| + \sum_{k_R} E_{k_R}^\sigma |k_R\sigma\rangle\langle k_R\sigma| + \sum_{k_L} E_{k_L}^\sigma |k_L\sigma\rangle\langle k_L\sigma| + \sum_{k_a} E_{k_a}^\sigma |k_a\sigma\rangle\langle k_a\sigma| \\ & + \sum_{k_a} \left[V_{Dk_a}^\sigma |D\sigma\rangle\langle k_a\sigma| + V_{k_aD}^\sigma |k_a\sigma\rangle\langle D\sigma|\right] + \sum_{k_a} \left[V_{Ak_a}^\sigma |A\sigma\rangle\langle k_a\sigma| + V_{k_aA}^\sigma |k_a\sigma\rangle\langle A\sigma|\right] \\ & + \sum_{k_L} \left[V_{Dk_L}^\sigma |D\sigma\rangle\langle k_L\sigma| + V_{k_LD}^\sigma |k_L\sigma\rangle\langle D\sigma|\right] \\ & + \sum_{k_R} \left[V_{Ak_R}^\sigma |A\sigma\rangle\langle k_R\sigma| + V_{k_RA}^\sigma |k_R\sigma\rangle\langle A\sigma|\right] \qquad (1)\end{aligned}$$

The index k_i is the energy wave vector, with i represents the indexes D, A, a, L and R. E_i^σ represents the ith energy level position and spin. $|i\sigma\rangle$ and $\langle j\sigma|$ represent the ket and bra states, respectively. Vij

represents the coupling interaction between the subsystems *i* and *j* with V*ij*= V*ji*. The system time dependent and spin dependent wave function can be written as,

$$\Psi^{\sigma}(t) = C_D^{\sigma}(t)|D\sigma\rangle + C_A^{\sigma}(t)|A\sigma\rangle + \sum_{k_a} C_{k_a}^{\sigma}(t)|k_a\sigma\rangle + \sum_{k_L} C_{k_L}^{\sigma}(t)|k_L\sigma\rangle + \sum_{k_R} C_{k_R}^{\sigma}(t)|k_R\sigma\rangle \quad (2)$$

Where, C_j^{σ}(t) represents the linear expansion coefficients, with j=D, A, a, L and R. The equations of motion for C_j^{σ}(t) can be obtained by using time dependent Schrodinger equation [7] (in atomic units):

$$\frac{\mathrm{d}\Psi^{\sigma}(\mathrm{t})}{\mathrm{dt}} = -i\hat{H}\Psi(t) \quad (3)$$

For steady state case, we define $C_j^{\sigma}(t)$ as $C_j^{\sigma}(t) = \bar{C}_j^{\sigma}(E^{\sigma})\, e^{-iE^{\sigma}t}$ with E^{σ} represents the spin dependent system energy. For steady state, we have $\frac{\mathrm{d}C_j^{\sigma}}{\mathrm{dt}} = 0$ and by using the suitable separation procedure; $V_{k_j\alpha}^{\sigma} = \upsilon_{k_j}^{\sigma} V_{i\alpha}^{\sigma}$ *and* $\bar{C}_{k_I}^{\sigma} = \upsilon_{kI}^{\sigma}\bar{\bar{C}}_I^{\sigma}$,we get the following set of time dependent and spin dependent related equations,

$$\bar{C}_D^{\sigma}(E^{\sigma}) = \frac{1}{E^{\sigma} - E_D^{\sigma}}\left\{V_{DL}^{\sigma}\sum_{k_L}|\upsilon_{k_L}^{\sigma}|^2\bar{\bar{C}}_L^{\sigma}(E^{\sigma}) + V_{Da}^{\sigma}\sum_{k_a}|\upsilon_{k_a}^{\sigma}|^2\bar{\bar{C}}_a^{\sigma}(E^{\sigma})\right\} \quad (4)$$

$$\bar{C}_A^{\sigma}(E^{\sigma}) = \frac{1}{E^{\sigma} - E_A^{\sigma}}\left\{V_{AR}^{\sigma}\sum_{k_R}|\upsilon_{k_R}^{\sigma}|^2\bar{\bar{C}}_R^{\sigma}(E^{\sigma}) + V_{Aa}^{\sigma}\sum_{k_a}|\upsilon_{k_a}^{\sigma}|^2\bar{\bar{C}}_a^{\sigma}(E^{\sigma})\right\} \quad (5)$$

$$\bar{\bar{C}}_a^{\sigma}(E^{\sigma}) = \frac{1}{E^{\sigma} - E_a^{\sigma}}\left\{V_{aD}^{\sigma}\bar{C}_D^{\sigma}(E^{\sigma}) + V_{a_A}^{\sigma}\bar{C}_A^{\sigma}(E^{\sigma})\right\} \quad (6)$$

$$\bar{\bar{C}}_L^{\sigma}(E^{\sigma}) = \frac{1}{E^{\sigma} - E_L^{\sigma}}V_{LD}^{\sigma}\bar{C}_D^{\sigma}(E^{\sigma}) \quad (7)$$

$$\bar{\bar{C}}_R^{\sigma}(E^{\sigma}) = \frac{1}{E^{\sigma} - E_R^{\sigma}}V_{RA}^{\sigma}\bar{C}_A^{\sigma}(E^{\sigma}) \quad (8)$$

Then, by using the following definition of the self- energy [8]:

$$\sum\nolimits_{ij}^{\sigma}(E^{\sigma}) = \left|V_{ij}^{\sigma}\right|^2\Gamma_j^{\sigma}(E^{\sigma})\,;\ \Gamma_{i(E)} = \sum_{ki}\frac{|\upsilon_{ki}|^2}{E - E_i} \quad \text{where}$$

$$\Gamma_j^{\sigma}(E^{\sigma}) = -i\pi\rho_j^{\sigma}(E^{\sigma}) + P\int\frac{\rho_j^{\sigma}(E^{\sigma})dE'^{\sigma}}{E^{\sigma} - E'^{\sigma}} \quad (9)$$

and the spin dependent density of states is given by $\rho_j^{\sigma}(E^{\sigma}) = \sum_{k_j}\left|\upsilon_{k_j}^{\sigma}\right|^2\delta\left(E_{k_j}^{\sigma} - E^{\sigma}\right)$

By substituting eq. (6) and eq. (8) in equation (5), then eq. (5) can be written as:

Now, the spin dependent the transmission amplitude and transmission probability can be respectively defined by: $t^{\sigma}(E^{\sigma}) = \frac{\bar{C}_A^{\sigma}(E^{\sigma})}{\bar{C}_D^{\sigma}(E^{\sigma})}$ and $\tau^{\sigma}(E^{\sigma}) = |t^{\sigma}(E^{\sigma})|^2$

The eigen values of the active region, that contains base pairs with backbone (when the base pairs arranged in homogenous sequence) will be calculated by using tight binding model [7]:-

$$E_j^{\sigma} = E_{basis} - 2t_{bp}^{\sigma}\cos\left(\frac{\pi j}{N+1}\right) \pm \sqrt{\left[t_{bp}^{\sigma}\cos\left(\frac{\pi j}{N+1}\right)\right]^2 + 2{t_{bb}^{\sigma}}^2} \quad (10)$$

Where j refers to single base pair. E_{basis} is the energy of the basis (i.e the energy of one base pair). N(=10) represents the number of the base pairs. t_{bp} is the coupling interaction between nearest-neighbor base pairs. t_{bb} is the coupling interaction between base pairs and backbone. In the presence of magnetic field and spin dependent coupling interaction between subsystems, the eigen values become: $E_j^{\sigma} \rightarrow E_j^{\sigma} + \sigma\Delta_s$; where $\sigma = \pm 1$ for spin up and spin down, respectively. Δ_s represents the energy splitting due to magnetic field effect. $E_j^{\sigma}\,(E_j^{-\sigma})$ represents the spin up (down) energy orbitals of the DNA active region. It is obvious that the accumulation of spin up electrons in leads is greater than the accumulation of spin down electrons. Extended programs based on Fortran language are accomplished to calculate all the spin transport properties for all applied parameters that considered in our model calculation in both cases of Leads spin configuration in the presence and absence of spin orbit Coupling.

3. Calculations and Results

All the electronic and transport properties will be calculated and studied for the case of leads in the parallel configuration. μ_{α}^{σ} represents the chemical potential of the lead $\alpha(= \mathrm{L}, \mathrm{R})$ for certain spin σ . $\mathrm{E_A^{\sigma}(E_D^{\sigma})}$ represents the spin dependent energy levels of the accepter (donor). For this case, we have $\mu_{\mathrm{L}}^{\sigma} = \mu_{\mathrm{R}}^{\sigma} = 0.1$ eV and $\mu_{\mathrm{L}}^{-\sigma} = \mu_{\mathrm{R}}^{-\sigma} = -0.1$ eV.
Firstly, our calculations are accomplished for two regimes, the strong regime where $\mathrm{t_{bb}^{\sigma} > t_{bp}^{\sigma}}$, the weak regime where $\mathrm{t_{bb}^{\sigma} < t_{bp}^{\sigma}}$ It is experimentally well known that, the coupling interaction between base pairs and backbone simulates environmental effects. Accordingly, the case "Without" backbone must be also studied. Firstly, the (G/C)10 active region eigen energy values and the spin dependent transmission spectrum are calculated for $\mathrm{t_{bb}^{\pm\sigma} = 0}$ .. The basepaire–backbone coupling interactions for the upper and lower backbone sites (for certain spin) are considered in all our treatment to be equal. The parameters used in our calculations for the case of strong regime are: $\mathrm{t_{bp}^{\sigma} = 0.5eV}$, $\mathrm{t_{bp}^{-\sigma} = 0.25eV}$, $\mathrm{t_{bb}^{\sigma} = 0.7eV}$ and $\mathrm{t_{bb}^{-\sigma} = 0.35eV}$, while for the case of weak regime $\mathrm{t_{bp}^{\sigma} = 0.7eV}$, $\mathrm{t_{bp}^{-\sigma} = 0.35eV}$, $\mathrm{t_{bb}^{\sigma} = 0.5eV}$ and $\mathrm{t_{bb}^{-\sigma} = 0.25eV}$. The coupling interactions between subsystems are $\mathrm{V_{AR}^{\sigma} = 1.5eV}$, $\mathrm{V_{AR}^{-\sigma} = 0.75eV}$, $\mathrm{V_{Aa}^{\sigma} = 1.2eV}$, $\mathrm{V_{Aa}^{-\sigma} = 0.6eV}$, $\mathrm{V_{aD}^{\sigma} = 0.5eV}$ and $\mathrm{V_{aD}^{-\sigma} = 0.25eV}$. The energy levels of the accepter quantum contact are $\mathrm{E_A^{\sigma} = -0.2eV}$, $\mathrm{E_A^{-\sigma} = 0.2eV}$, $\mathrm{E_D^{\sigma} = 0.7eV}$ and $\mathrm{E_D^{-\sigma} = 0.35eV}$ To accomplish our calculations the eigen values of the active region are calculated for the sequence (G/C)10 for all regimes by using eq.(10) in the presence of applied magnetic field. $\mathrm{E_{basis}}\left(= \frac{\mathrm{E_G + E_C}}{2}\right)$ is the energy of one base pair [9]. $\mathrm{E_G}(= -0.63\mathrm{eV})$ and $\mathrm{E_C}(= -3.75\ \mathrm{eV})$ are the onsite energies of Guanine and Cytosine, which are calculated with respect to $\mathrm{E_F} = -5.5$ eV. The energy levels of the active region are presented in table (1) for the case of strong, weak and without backbone regimes, respectively.

Table 1. The energy eigen values of the (G/C)10 for the strong and weak regimes as well as the without backbone regime.

Strong Regime $E_j^{\sigma}, E_j^{-\sigma}$ (eV)	Weak Regime $E_j^{\sigma}, E_j^{-\sigma}$ (eV)	"without" backbone $E_j^{\sigma}, E_j^{-\sigma}$ (eV)
2.4495	2.7085	2.4049
2.3068	2.4879	2.1566
2.0875	2.1494	1.7652
1.8169	1.7361	1.2623
1.5248	1.1492	0.9974
1.2401	1.3033	0.8733
1.0197	1.0389	0.6888
0.9860	0.9048	0.6776
0.9484	0.8697	0.4261
0.8387	0.6630	0.1394
0.7783	0.5729	0.0992
0.7034	0.4466	-0.0221
0.6243	0.3158	-0.0498
0.5574	0.2474	-0.0684
0.5305	0.1324	-0.1553
0.4150	0.0814	-0.1988
0.2880	0.0219	-0.2392
0.1839	-0.0470	-0.2816
0.1071	-0.1387	-0.3044
0.0602	-0.1940	-0.3458

For the case of strong regime, the spin up eigen values are lying in the regime 0.5305 $eV \leq E_j^{\sigma} \leq$ 2.4495 eV , while the spin down values are lying 0.0602eV $\leq E_j^{-\sigma} \leq 1.0197\ eV$. And for the case of weak regime, the spin up eigen values are lying in the regime $0.0219eV \leq E_j^{\sigma} \leq 2.7085\ eV$, while the spin down values are lying -0.1940$eV \leq E_j^{-\sigma} \leq 1.1492eV$. Table (3-2) presents the values of spin up energy levels $-0.2816eV \leq E_J^{\sigma} \leq 2.4049eV$ and the spin down energy levels $-0.3458eV \leq E_J^{-\sigma} \leq 0.99749eV$. The of $E_J^{\sigma}(E_J^{-\sigma})$ are shifted to the higher (lower) energy spectrum. All these energies are LUMO orbitals. The eigen values of the sequence (G/C)10 are utilized to calculate the transmission spectrum for strong and weak regimes. Fig. (2) represents the transmission spectrum for both spin in the strong regime. The transmission probability for spin up is higher than that of spin down.Also, the number of resonances for spin up transmission probability equals to 9(=N-1), while for spin down it is nearly equal to 7 . The spin up (spin down) transmission spectrum is (is not) shifted towards the higher energies. The number of peak-dip transmissions changes with spin. These resonances may be called Fano-resonances which emerge because of quantum interference effects. Experimentally, the coupling interaction between base pairs and backbone corresponds to the environmental variations. The transmission spectrum for the weak regime is shown in Fig.(3). The transmission probability becomes higher as the coupling interaction between the base pairs and backbone is lower than the coupling interaction between the base pairs. The transmission spectrum for both spin are nearly located at the same rang of energy, bearing in mind that the spin up accumulation in the leads is the higher one. As the backbone – base pair interaction is neglected, the number of resonances reduces to 7 for spin up channel and to 4 for spin down channel (see Fig.(4)). The spin dependent transmission spectrum is employed to calculated the spin dependent current that transports through the (G/C)10 active region. The spin current through the active region (base pairs with backbones) is calculated according to Landauer transport formula[10]; $I^{\sigma} = \frac{2e}{h}\int_{-\infty}^{+\infty} \tau^{\sigma}(E)[f_L^{\sigma}(E) - f_R^{\sigma}(E)]\, dE$. $f_{\alpha}^{\sigma}(E)$ is the spin dependent

Fermi distribution function of σ spin electrons in the lead α (=L,R) : $f_\alpha^\sigma(E) = \left\{1 + \exp\left[\frac{E-\mu_\alpha^\sigma}{k_B T_\alpha}\right]\right\}^{-1}$. T_α is the lead temperature and k_B is Boltzmann constant. Then by applying bias voltage eV_b on both leads , the chemical potentials become for left and right leads $\left(\mu_L^{\pm\sigma} + \mathrm{e}V_b\right)$and $\left(\mu_R^{\pm\sigma} - \mathrm{e}V_b\right)$. Accordingly , the spin up energy window will be $(\mu_L^\sigma + \mathrm{e}V_b) \leq W_E^\sigma \leq (\mu_R^\sigma - \mathrm{e}V_b)$, while the spin down one will be $(\mu_L^{-\sigma} + \mathrm{e}V_b) \leq W_E^{-\sigma} \leq (\mu_R^{-\sigma} - \mathrm{e}V_b)$. The spin dependent currents ($I^\sigma and\, I^{-\sigma}$) are calculated for $-1.0\ \mathrm{e}V \leq \mathrm{e}V_b \leq 1.0\ \mathrm{e}V$ with $T_R = T_L = 300K$, which means that the case of thermal equilibrium is considered. Our calculations are presented for both regime in Figs.(5) and (6). Fig.(5) shows spin blockade effect in I^σ and $I^{-\sigma}$ curves. For spin up , the spin blockade voltage eV_{SB}^σ equals 0.79eV, while for spin down $eV_{SB}^{-\sigma}$=0.21eV. Also $I^\sigma(I^{-\sigma})$ shows linear I^σ_ eV_b ($I^{-\sigma}$_ eV_b) relation for $|\mathrm{e}V_b| > 0.3955\mathrm{e}V$ (0.1038eV) , where $I^{-\sigma} > I^\sigma$.

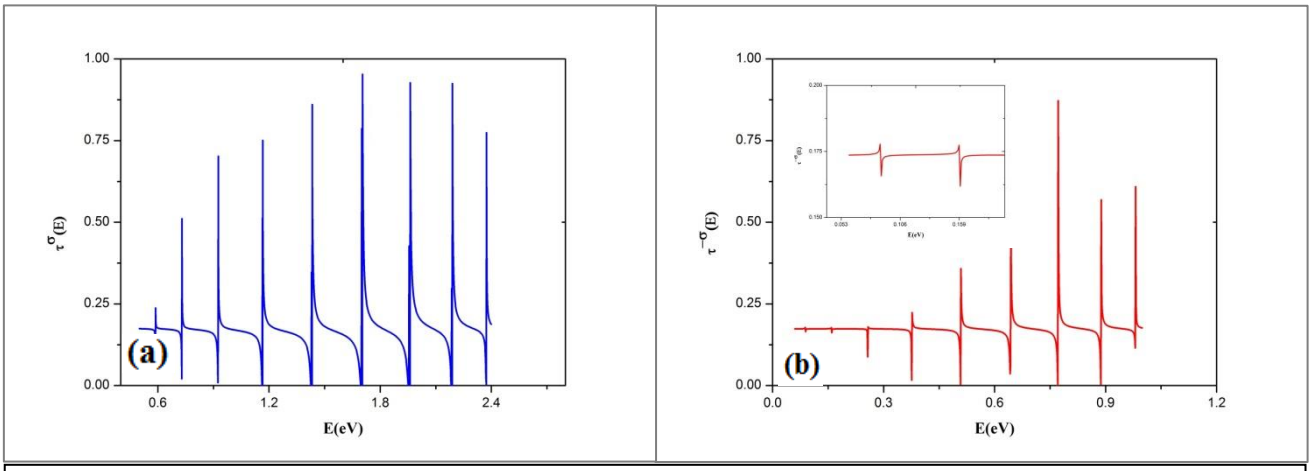

Fig (2): τ^σ and $\tau^{-\sigma}$ spectrum for the strong regime (G/C)10.

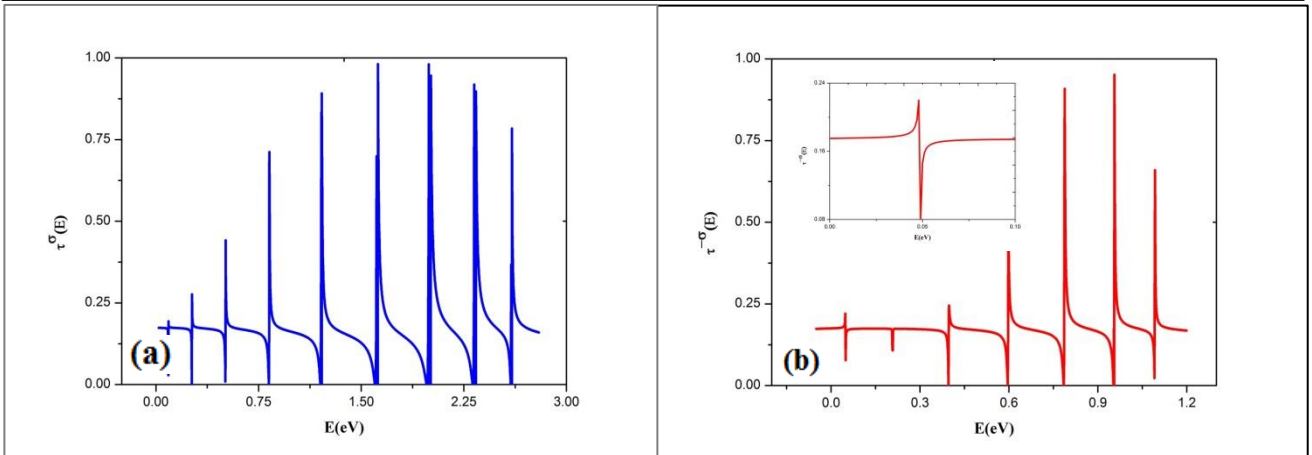

Fig (3): τ^σ and $\tau^{-\sigma}$ spectrum for the weak regime (G/C)10.

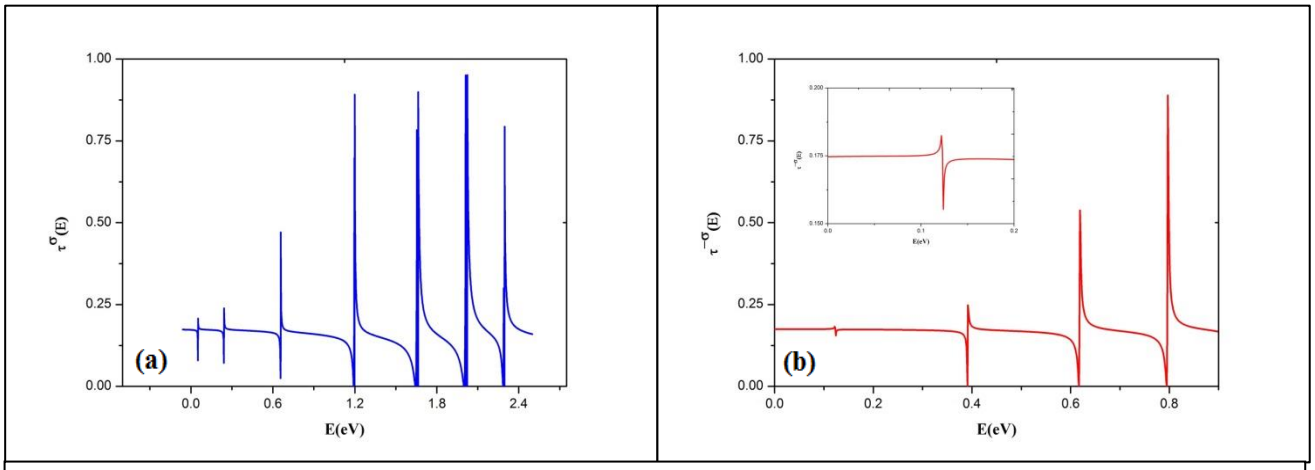

Fig.(4): τ^{σ} and $\tau^{-\sigma}$ spectrum for the "Without" Backbone regime (G/C)10.

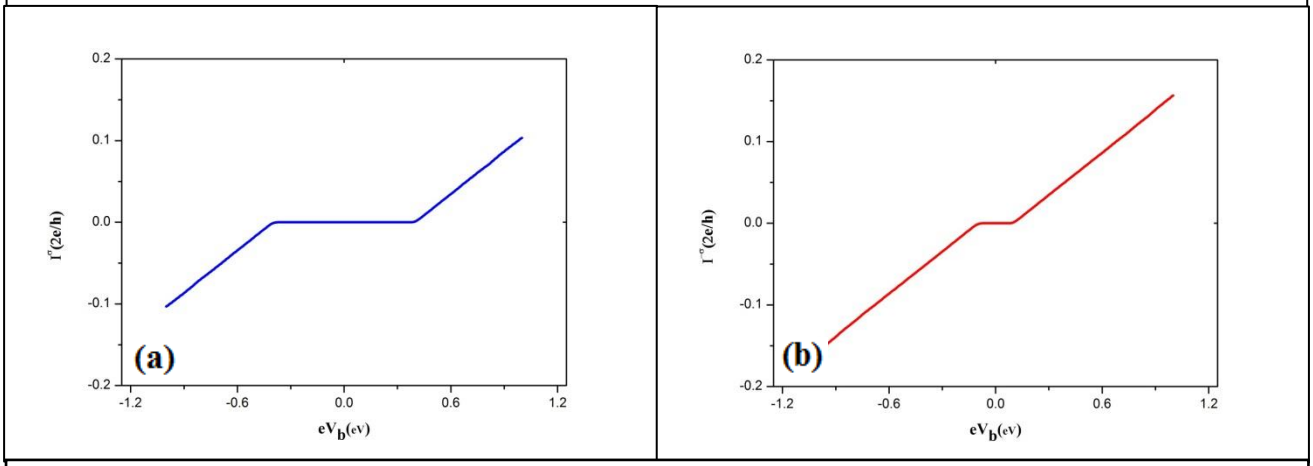

Fig.(5): The spin – dependent current as a function of bias voltage for the strong regime (G/C)10.

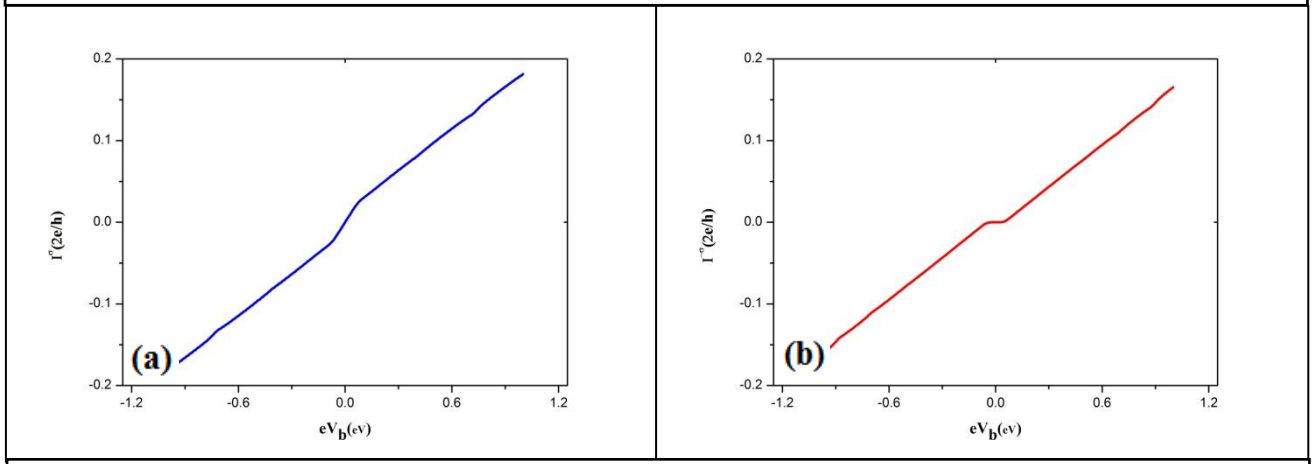

Fig.(6): The spin – dependent current as a function of bias voltage for the weak regime(G/C)10.

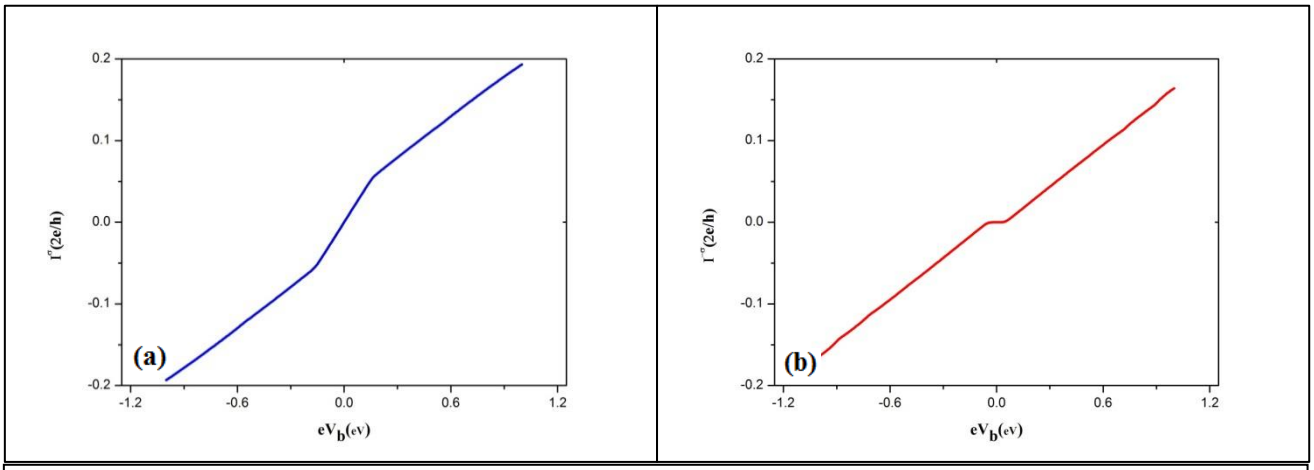

Fig.(7): The spin – dependent current as a function of bias voltage for the "Without" Backbone

Not the same features can be reported for the weak regime. In Fig (6), the spin up dependent current show three linear relations. No spin up blockade is noticed, while narrow spin down blockade is obvious. In general, shows nearly equal values of I^{σ} and $I^{-\sigma}$ for certain bias voltage. All these reported features are due to the resonances position (*i.e* LUMO levels) if they are lying with in the energy window or out of it. Fig.(2) shows that the spin up resonances are lying nearly out the spin up energy window. While the spin down resonances are lying within it. So, for strong regime ,we have $eV_{SB}^{\sigma} > eV_{SB}^{-\sigma}$, while for weak regime , no spin blockade is noticed. Certainly , the spin transport properties are determined by the number of spin dependent resonances and their position with respect to the spin dependent energy window $W_E^{\pm\sigma}$. In Fig.(7), in general $I^{\sigma}$is nearly equal $I^{-\sigma}$, but I^{σ} shows three range of bias voltage, in all the relation $I^{\sigma} - eV_b$ is linear. While $I^{-\sigma}$ shows spin down blockade in the range $-0.045eV < eV_b < 0.045eV$, i.e $eV_{SB}^{-\sigma} = 0.09eV$.The spin dependent conductance is also calculated using the following formula [10]. $G^{\sigma} = \frac{2e^2}{h}\int_{-\infty}^{+\infty} dE\ \tau^{\sigma}(E)\frac{\partial f^{\sigma}(E)}{\partial E}$. The spin dependent conductance are presented in Figs.(6) and (7) as function of $10K < T_{\alpha} < 300K$ for strong and weak regimes , respectively. In Fig. (6) , one can notice that G^{σ} is independent of temperature for $T < 225K$, while for $T > 275K$ the relation of G^{σ} with T_{α} becomes linear. Also , it is observed that $G^{-\sigma} \gg G^{\sigma}$. In the weak regime , G^{σ} and G^{σ}decreases with temperature increasing , One of the most important feature is $G^{\sigma} \gg G^{-\sigma}$, The enhancement in the values of conductance, in the case of weak regime, may be attributed to the increase of the hybridization between the accepter energy levels with active region energy levels. With increasing temperature, the spin up conductance shows nearly constant value, while $G^{-\sigma}$ increases linearly as $T > 125K$ (see Fig.(10)).

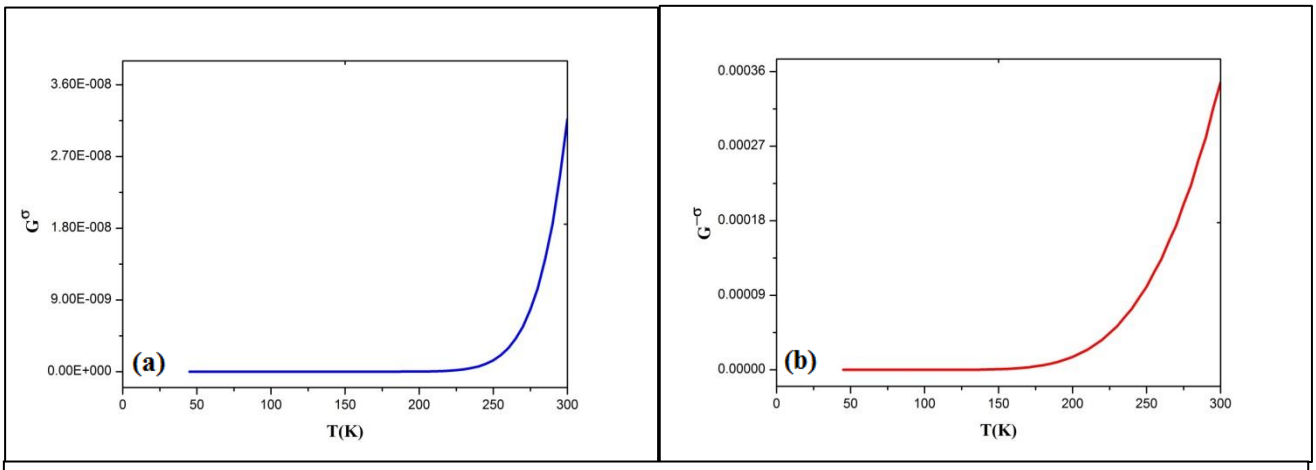

Fig.(8): The spin – dependent conductance as a function of temperature for the strong regime

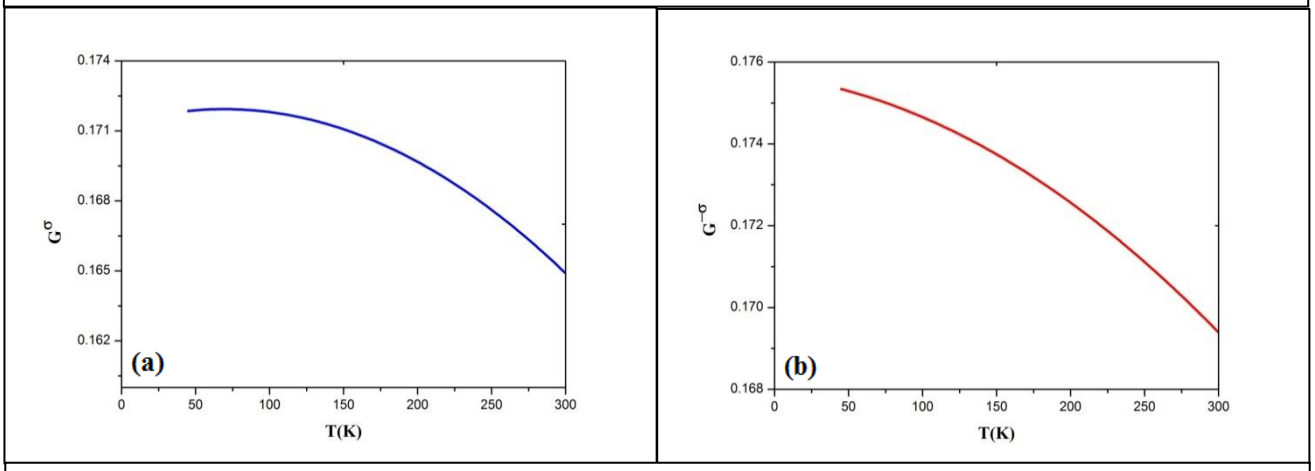

Fig.(9): The spin – dependent conductance as a function of temperature for the weak regime

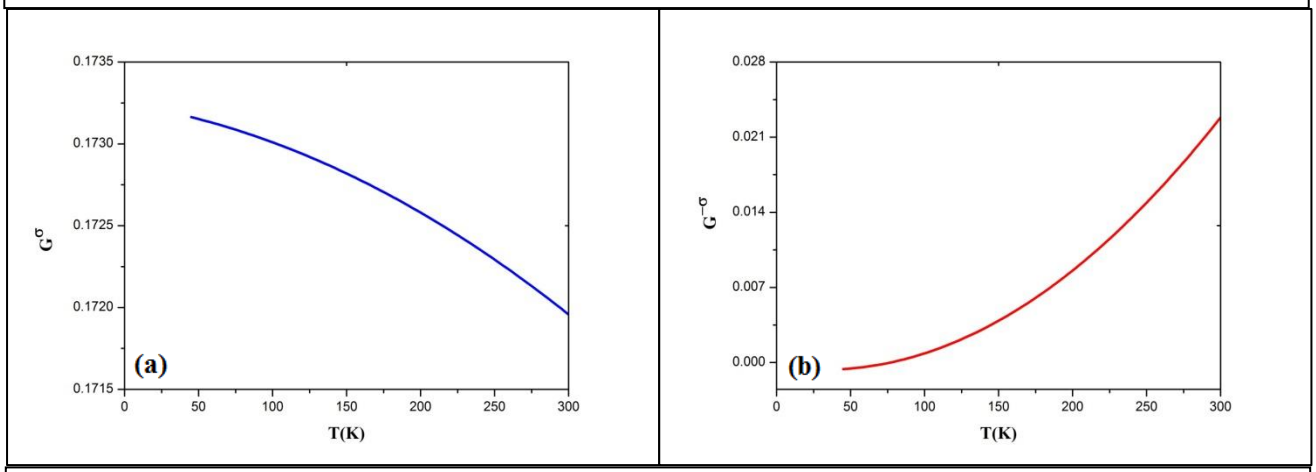

Fig.(10): The spin – dependent conductance as a function of temperature for the "without"

4. Conclusions

In our study, we investigate the effect of spin on the electron transport through a certain number of base pairs when exposed to the variations of the coupling between (FM-(G/C)10-FM) subsystems, *ie* the spin dependent quantum contacts and leads and the effect of backbone. The spin transport properties through (G/C)10 are evaluated numerically. In relation to the spin dependent feature applications, we

dealt with several parameters associated with the experimental works. (G/C)10 sequences have been employed to determine the spin transmission and $I^{\sigma}\_eV_b$ characteristic in the absence of spin-orbit coupling. Our results, that are summarized in table (2), have described various features of the (G/C)10 molecule. Our calculations include the characteristics of the structures and their relevance to the spin transport properties. We found that the spin-polarized current could rapidly increase under a small bias voltage by tuning the coupling interactions between the subsystems. We also focused our attention to the impact of temperature on the spin transport properties. Increasing temperature may cause the destruction of the phase coherence and may lead to the reduction of conductance. It is concluded that the (G/C)10 structures are good for spin filter applications. Their structures produce effective quantum confinement, thus (G/C)10 structures may be excellent candidates for the spintronics applications such as spin switching.

Finally, for future analysis, we need to study the spin filtration efficiency of (G/C)N for the case of antiparallel leads-configuration.

Table 3. summarizes the physical features of I^{σ} and $I^{-\sigma}$

$\Delta_{SO}= 0.0$		
	Parallel configuration	**Antiparallel configuration**
Strong regime	.$V_{SB}^{\sigma} > V_{SB}^{-\sigma}$ $V_{SB}^{\pm\sigma}$ increase with the molecular length. $I^{\sigma} < I^{-\sigma}$	.$V_{SB}^{\sigma} > V_{SB}^{-\sigma}$ $V_{SB}^{\sigma}(V_{SB}^{-\sigma})$is shifted to the negative (positive) bias voltage. $I^{\sigma} < I^{-\sigma}$
Weak regime	is linear with eV_b, $I^{-\sigma}$shows I^{σ} spin blockade both are symmetric with eV_b=0 $I^{\sigma} > I^{-\sigma}$	) ,is linear with eV_b, shifted to $I^{\sigma}(I^{-\sigma}$ the negative (positive) bias voltage. $I^{-\sigma} > I^{\sigma}$
Without backbone	is linear with eV_b. is also linear with $I^{-\sigma}$, except for N = 10 both are eV_b symmetric with eV_b. $I^{\sigma} \approx I^{-\sigma}$	) is linear with eV_b; shifted to $I^{\sigma}(I^{-\sigma}$ the negative (positive) bias voltage. $I^{-\sigma} > I^{\sigma}$

5. References

[1] Z. Zhang, Y. Wang, H. Wang, H. Liu, L. Dong, "Controllable Spin Switching in a Single-Molecule Magnetic Tunneling Junction," Nanoscale Res Lett., vol. 16, no. 1, 2021.Doi:https://doi.org/10.1186/s11671-021-03531-0

[2] M. Ratner, "Introducing molecular electronics," J. Chem.phys, vol. 5, no. 154, Nov 2021.Doi:https://doi.org/ 10.1016/S1369-7021(02)05226-4

[3] S. Abdalla, A. Obaid, F. M. Al-Marzouki, "Effects of Environmental Factors and Metallic Electrodes on AC Electrical Conduction Through DNA Molecule," Nanoscale Res Lett, vol. 12, 2017.Doi:https://doi.org/10.1186/s11671-017-2076-y

[4] R. Gutiérrez, S. Mandal, G. Cuniberti, “Dissipative effects in the electronic transport through DNA molecular wires,” Phys Rev B Condens Matter Mater Phys Rev, vol. 71, no. 23, Jun. 2005.Doi:https://doi.org/10.1103/PhysRevB.71.235116

[5] J. Hihath, B. Xu, P. Zhang, N. Tao, “Study of single-nucleotide polymorphisms by means of electrical conductance measurements,” Proc Natl Acad Sci U S A, vol. 102, no. 47, pp. 16979–16983, Nov 2005.Doi:https://doi.org/10.1073/pnas.0505175102

[6] D. Porath, A. Bezryadi, S. de Vries, C. Dekker “Direct measurements of electrical transport through DNA molecules,"AIP Publishing, vol. 544, no. 452, (2000).Doi:http://dx.doi.org/10.1063/1.1342553

[7] A. Al-Saidi, J. Al-Mukh, S. I. Easa. of Basrah, and undefined, “Steady State Formalism for Electron Transfer through DNA System: Fishbone Model," IJSR, vol. 3, no. 10, Oct 2014.Doi:https://doi.org/: 14190 /. IJSR. 2319-7064

[8] A. T. Ibrahim, J. AL-Mukh , "The Electron Transport Properties of Qubit Coupled with SET The Tuning of the Qubit Energy Levels," JBRS, vol, 45, no. 1, 2019.

[9] D. Klotsa, R. A. Ro¨mer, M. S. Turner, "Electronic Transport in DNA," Biophysical Journal, vol. 89, Oct 2005.Doi:https://doi.org/10.1529/biophysj.105.064014

[10] Y. A. Berlin, A. l. Burin, M. A. Ratner, " On the Long-Range Charge Transfer in DNA,"J. Phys.Chem. A, vol. 104, No. 3, Jan 2000.Doi:https://doi.org/10.1021/jp9933323

Journal of Basrah Researches (Sciences) **50**(1), 62 (2024)
DOI: https://doi.org/10.56714/bjrs.50.1.6

دراسة نظرية لنقل البرم خلال جزئ الحمض النووي الموضوع بين قطبين فيرومغناطيسيين.

مهند محسن مرزوك، جنان مجيد المخ*

قسم الفيزياء، كلية التربية للعلوم الصرفة، جامعة البصرة، البصرة، العراق.

معلومات البحث

الاستلام 25 تشرين الثاني 2023
القبول 13 شباط 2024
النشر 30 حزيران 2024

الكلمات المفتاحية

نقل البرم خلال جزئ (G/C)10 , قطبين فيرومغناطيسيين , ترشيح برم , تبديل برم, حصار البرم.

Citation: M.A. Merzoq, J.M. Al-Mukh, J. Basrah Res. (Sci.) **50**(1), 62 (2024). DOI:https://doi.org/10.56714/bjrs.50.1.6

الملخص

في هذه الدراسة، نقترح نموذجًا فيزيائيًا لدراسة نقل البرم عبر نظام الحمض النووي وتوفير آلية فيزيائية واضحة للظاهرة المعتمدة على البرم. النظام قيد الدراسة هو قواعد الحمض النووي كوانين-سايتوسين مقترنة بقطبين مغنطيسيين (FM-(G/C)10-FM) في حالة توزيع التوازي وضديد للتوازي، بوجود نقاط اتصال كمية. تعتمد معالجتنا على انموذج الترابط المتين لاستخراج صيغة واضحة لطيف النفاذية الذي يتم استخدامه لفحص خصائص التيار المعتمد على البرم - جهد الانحياز وكذلك التوصيلية المعتمدة على البرم - درجة الحرارة. اجريت حساباتنا للنهج القوي والنهج الضعيف وكذلك للنهج بدون العمود الفقري. هناك عوامل مختلفة تشارك في دراستنا, الاتصالات الكهربائية بين جزيئات الحمض النووي والأقطاب الكهربائية، وبنية جزيء الحمض النووي والبيئة المحيطية بجزيء الحمض النووي. تشمل العوامل المعتمدة على برم النظام، والتي تم بحثها على نطاق واسع في دراستنا، الاقتران المعتمد على البرم بين الأنظمة الفرعية، والاتصالات الكمية بين المنطقة الفعالة والأقطاب المغناطيسية، وبرم الإلكترونات الاكثرية والاقلية في الاقطاب المغناطيسية وكذلك جهد الانحياز المطبق خارجيًا. يمكن أن يؤدي تباين هذه العوامل إلى تعزيز أو تخميد نقل البرم عبر جزيء (G/C)10. تتوافق حسابات طيف النفاذية مع نقل البرم في جميع أنحاء (G/C)10 حيث ينشأ من خلال عملية نفق متشاكه بين القواعد المتجاورة من خلال تداخل مدارات LUMO الخاصة بالقواعد. أظهرت النتائج التي توصلنا إليها أن نقل البرم المستقطب الذي يمكن تنظيمه بشكل فعال من خلال نوع النهج بالإضافة إلى توزيع البرم في الاقطاب والذي يمكن أن يظهر ترشيح برم فعال وتبديل البرم من خلال استخدام ظاهرة حصار البرم.

***Corresponding author email :** www.montader1999.mm@gmail.com

ISSN: 1817-2695 (Print); 2411-524X (Online)
Online at: https://jou.jobrs.edu.iq